1B.3

INTERACTIONS BETWEEN SIMULATED TROPICAL CYCLONES AND AN ENVIRONMENT WITH A VARIABLE CORIOLIS PARAMETER

By

Elizabeth A. Ritchie[1] and William W. Frank[2]

1. Introduction

Vertical wind shear has strong effects on both the structure and intensity of a tropical cyclone. Since the early 1960's when researchers first began to measure the tropical cyclone environment, it has been known that large amounts of vertical shear inhibit tropical cyclone intensification while low values of shear favor both the genesis and intensification (Gray 1975) of tropical cyclones. It has also been shown numerically that in the Atlantic Ocean easterly shear favors tropical cyclone development and westerly shear inhibits it (Tuleya and Kurihara 1981).

Recent studies have shown that the interactions between the tropical cyclone and the vertically sheared environment result in a persistent wave number one asymmetry in the vertical motion field develops, which in turn modulates convection (e.g., Jones 1995; Bender 1997; Frank and Ritchie 2001, Halverson et al. 2006). The strongest convection occurs in the downshear-left sector of the storm (see Frank and Ritchie (2001) – their Fig. 9). Frank and Ritchie (2001) relate the weakening of the tropical cyclone under shear to a disruption in the tropical cyclone structure by 1) the advection of the upper-level structure of the tropical cyclone, 2) the effect of less optimal eye warming forced by asymmetrically organized convection, and 3) outward mixing of moist static energy from the eye and eyewall by transient eddies in the upper levels.

In an environment with a variable Coriolis parameter, a persistent vertical wind shear may exist over the tropical cyclone center due to the so-called "beta gyres". These gyres are produced by advection of planetary vorticity by the storm circulation causing a region of anomalously low vorticity to develop NE of the cyclone center and a positive anomaly to develop SW of the cyclone center (e.g., Chan and Williams 1987; Fiorino and Elsberry 1989). These gyres give the tropical cyclone a general propagation vector to the northwest (southwest) in the northern (southern) hemisphere. They also may give rise to vertical wind shear over the core of the tropical cyclone because of the variation with height of the primary circulation from cyclonic in the low levels to anticyclonic aloft. In the case of a tropical cyclone, the interaction with the planetary vorticity gradient will differ at different heights in the atmosphere resulting in a vertical wind shear across the tropical cyclone center. Frank and Ritchie (2002) postulated that if this "beta-shear" does exist and proves to be important in modulating the structure of the tropical cyclone, then it may well explain differences in the response of tropical cyclone intensification to westerly versus easterly shear regimes.

Here, the idealized simulations of Frank and Ritchie (2001) are extended to include the effects of a variable Coriolis parameter (*f*) as a first step toward more realistically representing the structure of vertical wind shear that is routinely observed in the tropical atmosphere. In particular, in order to understand why there might be an east-west directional bias for favorable tropical cyclone genesis conditions, it is important to understand the first-order effects of the gradient in planetary vorticity on tropical cyclone structure and intensity. Section 2 outlines the methodology used to set up the initial conditions for the two simulations presented in this paper. Results of the simulations are presented in section 3. A summary and discussion are presented in section 4.

2. Methodology

Two numerical simulations are performed that simulate the effects of planetary vorticity on a mature tropical cyclone. The model is version 5.3 of the Pennsylvania State University/National Center for Atmospheric Research (PSU/NCAR)

[1]Corresponding author address: Department of Electrical and Computer Engineering, MSC01 1100, 1 University of New Mexico, Albuquerque, NM 87131.

[2]The Pennsylvania State University

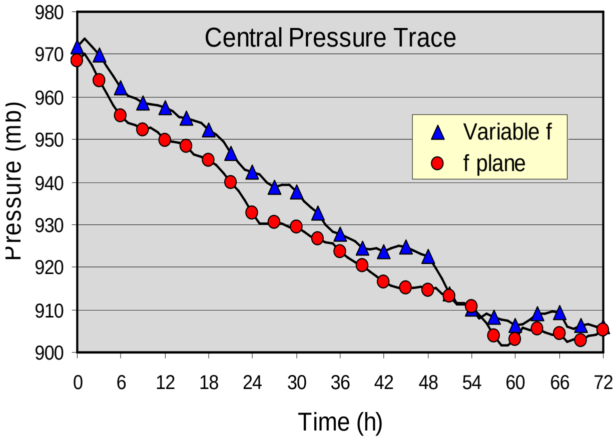

Figure 1: Time series of the minimum sea-level pressure for the beta-plane simulation (blue) and the f-plane simulation (red).

mesoscale model, and the configuration and physical parameterizations are the same as thatdescribed in Ritchie and Frank (2006). For both the simulations three nested domains are used with resolutions of 45-, 15-, and 5-km. The finest mesh is 700 km x 700 km and encompasses the inner-core region of the tropical cyclone. There are 23 vertical sigma levels. The model top is 50 mb, and a radiative boundary condition is used at the top of the model. Physical parameterizations include a Burk-Thompson boundary layer and Goddard explicit moisture scheme. No convective parameterization or radiative schemes are employed. The sea surface temperature (SST) is fixed at a uniform value of 28.5°C. The initial thermodynamic sounding is taken from the pre-storm cloud cluster composite of McBride and Zehr (1981), which was determined from rawinsonde data in the western North Pacific. The simulations are initialized with the same baroclinic vortex as that in Frank and Ritchie (2001) (not shown). It is axisymmetric with maximum winds of 15 m/s at a radius of 135 km - equivalent to a strong tropical depression. There is a broad anticyclone aloft, and the fields are in gradient balance. At the time of initialization there are no large-scale winds in the domain. For consistency with Frank and Ritchie (2001) the vortices are spun up for 48 h until the cloud processes are fully developed, one using constant *f* and one using variable *f*. The end of the spin-up time is called t = 0, and the runs are continued for a further 72-h until an approximate steady-state is observed. At t=0 both storms have central pressures of about 970 mb.

3. Results

3.1 Evolution of the tropical cyclone intensity

The central pressure traces from both simulations are shown in Fig. 1, and there is little difference in the evolution of the tropical cyclone intensity between the two simulations. Both simulations evolve steadily, with short periods of more intense development, particularly for the variable-*f* simulation. The constant-*f* simulation reaches a minimum intensity of 901 mb at about 58 h of simulation. The variable-*f* simulation intensifies a little more slowly, reaches a minimum pressure of about 906 mb by 60 h and approximately maintains that until 72 h. The difference in minimum pressure between the two simulations is never more than 10 mb throughout the 72-h of simulation. Although there is some difference in the evolution of the two cases, the effect on the intensity of the tropical cyclone is very small. In the following discussion, the constant-*f* and variable-*f* tropical cyclones will be referred to as the CFTC and VFTC respectively.

As would be expected from the minimum sea-level pressure traces, both simulated tropical cyclones undergo a fairly steady evolution of their wind and vorticity fields. Figure 2 shows the evolution of the azimuthally-averaged winds for both simulations. The CFTC winds initially increase more rapidly than the VFTC, similar to the development of the minimum sea-level pressure. However, by 48 h, both tropical cyclones are of similar strength in

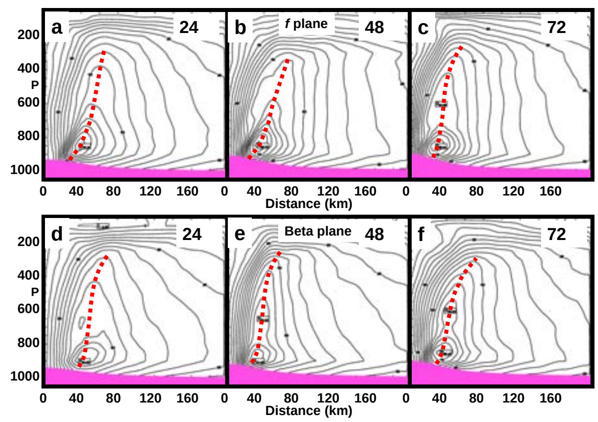

Figure 2: Azimuthally-averaged wind speed for a) – c) constant *f*; and d) – f) variable *f*. The RMW is indicated on all panels by the heavy dotted line. Wind speed contours are 5 m s^{-1}.

terms of their averaged wind field. The greatest radius of maximum winds (RMW) contraction in the constant-*f* simulation actually occurs in the middle levels of the tropical cyclone between 48 and 72 h as shown in Figs. 2a – 2c. In contrast, the RMW contraction in the variable-*f* simulation occurs mostly between 24 and 48 h at all levels. Subsequent to this, the structure of the VFTC becomes very asymmetric and the radius of maximum winds determined from the actual wind field expands, and is quite different in quadrants of the tropical cyclone (not shown).

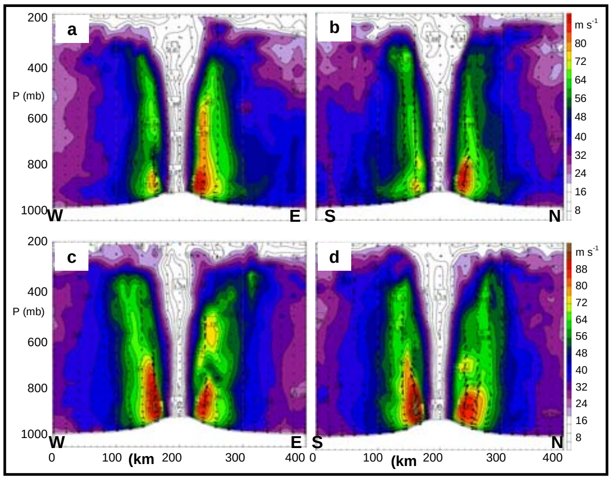

Figure 3: Vertical cross-sections of wind speed and in-plane circulation vectors at 48-h of simulation; a) variable *f* west-east; b) variable *f* south-north; c) constant f west-east; and d) constant f south-north.

Figure 3 shows south-north and west-east cross-sections of the tropical cyclones at 48 h of simulation. The most striking difference between the two simulations is the asymmetric structure of the wind field of the VFTC (Figs. 3a, 3b) compared with the CFTC (Figs. 3c, 3d). In particular, the winds on the west and south sides of the VFTC are much weaker than on the east and north sides. In addition, the overall size of the region of maximum winds is much greater for the CFTC than for the VFTC. For example, the region of winds greater than 48 m s^{-1} has been highlighted in figure 3 in green shades. This area is clearly greater in extent for the CFTC and more symmetrically structured when compared with the VFTC.

3.2 Evolution of the precipitation patterns

The area-averaged precipitation is calculated every 6 hours on a circle centered on the tropical cyclone minimum sea-level pressure. The 15-km resolution gridded data are interpolated to a cylindrical grid with 90 azimuthal points and a radial resolution of 5 km. Figure 4 shows a time trace of the area-averaged precipitation for both the variable-*f*, and constant-*f* simulations for circles of radius 100 km and 300 km. Figure 5 shows the evolution of the 6-h rainfall pattern for the constant-*f* and variable-*f* simulations respectively. The 100-km and 300-km radius averaging areas are indicated on Figs. 5a and 5d.

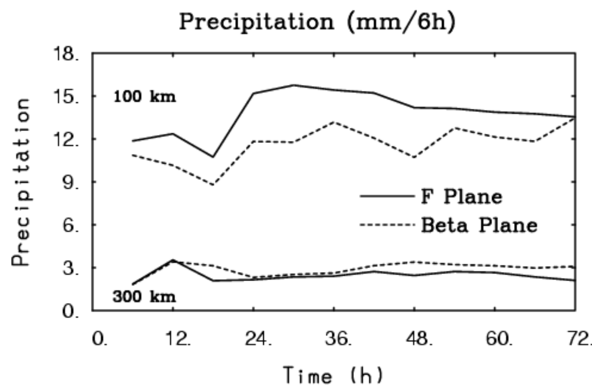

Figure 4: Area-averaged rainfall for the f (solid) and beta (dashed) plane simulations for a circle of radius of 100 and 300 km. The 100 and 300-km radius circles are indicated on Figure 5.

The overall amount of precipitation is fairly steady throughout both simulations, and the quantity of rainfall within 300 km is very similar (Fig. 4). However, the VFTC has a tendency for more rain farther from the center than the CFTC, which has the majority of its precipitation contained within 100 km of the center of the tropical cyclone in an intense, axisymmetric eyewall throughout the simulation (Figs. 5a – 5c). Although the VFTC simulation also has a majority of its precipitation located within the eyewall, the eyewall precipitation is very asymmetric with a maximum in the east-southeast quadrant at early times (Fig. 5d) and shifting to the east-northeast quadrant at later times (Figs. 5e, 5f). In addition, some precipitation is in a rainband located in the 100 to 300 km annulus to the east and south of the center of the tropical cyclone (Figs. 5d - 5f).

There is an apparent correlation between a decrease in the total amount of precipitation in the eyewall (Fig. 6) and a decrease in the rate of intensification (Fig. 1). This is particularly obvious in the VFTC simulation between 6 and 18 hours of simulation, 36 and 48 hours of simulation, and

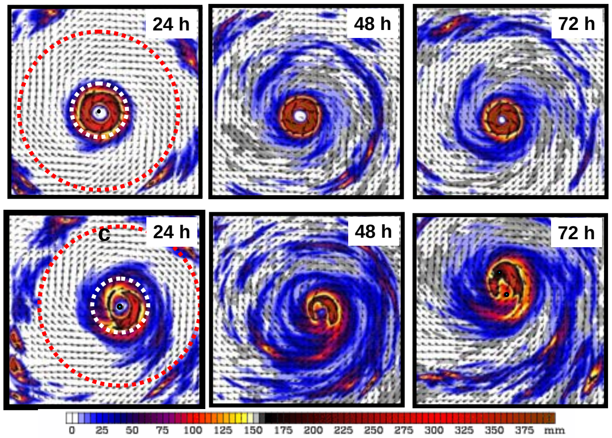

Figure 5. Sequence of 6-h rainfall on the 5-km grid. Top row - the f plane simulation; and bottom row - the beta plane simulation. The domain size is 700 x 700 km and surface wind vectors are also indicated.

again between 54 and 60 hours of simulation. The two latter time periods in the VFTC simulation correspond to two periods during which vertical wind shear (calculated as the difference in the average 200 and 850 mb winds) is above 9 m s^{-1}. In the case of the constant-*f* simulation, a brief lessening of the rate of intensification between 6 and 18 hours also corresponds to a drop in the total precipitation. Otherwise, the constant-*f* simulation divides into two longer time-scale episodes, one from 6-40 hours, when the rate of intensification is highest, and the magnitude of vertical wind shear is very low, and the other, from 40-72 hours when the rate of intensification is slightly less, the magnitude of vertical wind shear is slightly higher, the eye size rapidly decreases from 41 km to 20 km in diameter (measured by the zero rainfall contour), and the total precipitation in the eyewall steadily decreases (Fig. 4). This period corresponds to a period of rapid intensification (defined as > 1 mb h^{-1}) from 48 – 60 hours (Fig. 1) and also corresponds to the period of RMW contraction through the middle levels of the TC in Fig. 2.

3.3 The large-scale vertical wind shear

It is our main thesis that most of the differences between the evolution of the tropical cyclone using constant-*f* and that using variable-*f* are due to differences in the large-scale vertical wind shear that are generated by the interaction between the tropical cyclone circulation and its environment. To investigate this effect, the average environmental wind is calculated every 50 mb for 150-km, 300-km, 450-km, and 600-km radius circles centered on the tropical cyclone minimum sea level pressure. Similar to the calculation for precipitation in the previous section, the 15-km resolution gridded data are interpolated to a cylindrical grid with 90 azimuthal points and a radial resolution of 5 km. The calculations for the 300-km radius circle are presented here, since the average motion vector for that area best represents the actual motion of the simulated storms. Similar to accepted practice, the vertical wind shear is calculated as the difference between the averaged winds at 200 and 850 mb. Because there is little difference between the instantaneous calculation and the 6-h average shear, the instantaneous vertical wind shear is presented.

Figure 6 shows a representative plot of the average environmental wind, the 200-850 mb mean layer motion vector, and the shear vector calculated from 200 mb to 850 mb for each simulation. The calculated 850-200 mb mean motion vector is almost the same as the actual motion of each simulated TC (not shown). For the CFTC case, the average winds vary only very slightly through the simulation up to a height of about 400 mb (Fig. 6a). Above this, the average winds swing between southwesterly to northeasterly presumably because the anticyclonic outflow is less stable in structure than the cyclonic flow below due to migration of the upper-level rotational center (Wong and Chan 2004). The shear magnitude through this simulation varies from about 1 – 4 m s^{-1} (Fig. 7 - solid red dots).

As expected, there is considerably more structure in the averaged vertical winds for the VFTC case (Fig. 6b) because of the tropical cyclone

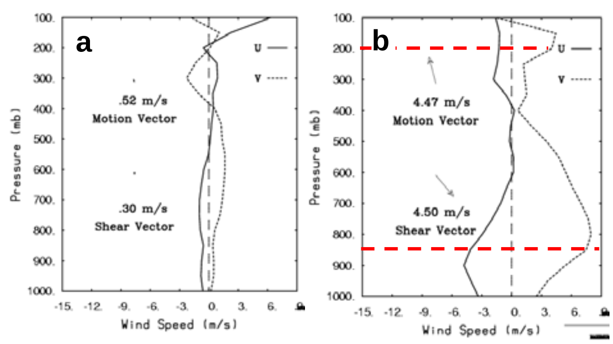

Figure 6: 72-h vertical profile of the mean u (solid) and v (dashed) components of the wind within 300km of the TC center. The mean layer motion between 200-850 mb, and the 200 - 850 mb shear vectors are indicated; a) the constant-*f* simulations; and b) the variable-*f* simulation.

interaction with the planetary vorticity gradient. A maximum in the averaged winds occurs near 850 mb similar to the jet reported by Bender (1997) for his simulations. The averaged winds weaken with increasing height, until at about 400 mb when they are essentially zero. Above 400 mb, the tropical cyclone winds turn anticyclonic and the interaction with the planetary vorticity gradient results in weak beta gyres of the opposite sense to those below.

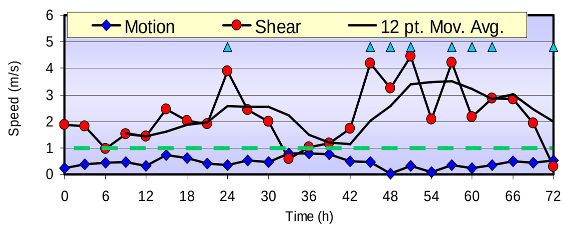

Figure 7: Time series of the magnitude of the TC motion and environmental shear for the f-plane simulation. The dashed line indicates the threshold shear magnitude for formation of rainfall asymmetries. The time when 1-h rainfall asymmetries formed are indicated by triangles.

If we plot horizontal maps of hourly rainfall for the constant-*f* simulation (e.g., Fig. 8) a clear trend develops. When the magnitude of the shear (Fig. 7) exceeds about 2.67 m s^{-1} (indicated by the dashed line in Fig. 7) then a wave-number-one asymmetry develops in the rainfall pattern (Figs. 8a, b). In general, the asymmetry is oriented between 30 and 60 degrees to the left (clockwise) of the direction the shear vector is pointing from. This locates the asymmetry in the downshear left half of the tropical cyclone, where an asymmetry would be expected if it was forced by the vertical wind shear (Frank and Ritchie 2001). This asymmetry develops in spite of the constant re-orientation of the direction of the shear vector that occurs throughout the constant-*f* simulation. Because the asymmetry is constantly shifting with the shear direction, a longer calculation of rainfall (e.g., 6-hourly) smears out the asymmetry and produces a more uniform band of rainfall around the eye (e.g., Fig. 5). When the shear magnitude is less than 2.67 m s^{-1}, asymmetries are sometimes observed, but not in a location expected from the shear direction.

From these results we conclude that a shear magnitude of at least 2.67 m s^{-1} calculated from 200 mb to 850 mb is required to force a corresponding persistent asymmetry in the cloud and rainfall pattern.

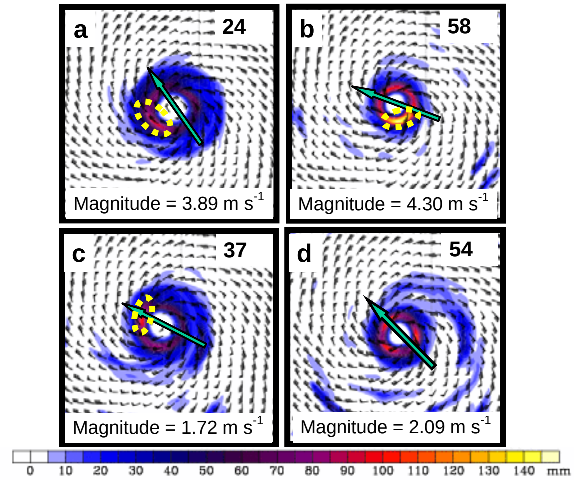

Figure 8: Examples of 1-h rainfall for a) and b) above-threshold shear; c) and d) below threshold shear with unrelated asymmetrys. The arrow indicates the direction of shear in each case.

At the start of the variable-*f* simulation, the calculated wind shear magnitude is about 7 m s^{-1}. It gradually intensifies reaching a peak value of 12 m s^{-1} before gradually relaxing back to 4.5 m s^{-1} by the end of the simulation (Fig. 9). Note that this apparently weak value of shear at 72-h of simulation corresponds to a time of very string 850-mb jet (Fig. 6b). However, because of the variability of the averaged wind structure above 400 mb, much of the strong shear from 850 to 400 mb is cancelled out. This may be an artifact of the way vertical wind shear is generally defined. If we ignore the outflow layer and calculate the shear between 300 and 850 mb, we find a slightly improved correlation between the shear magnitude and intensity trends (not shown). However, the improvement is not substantial enough to draw any definite conclusions at this stage.

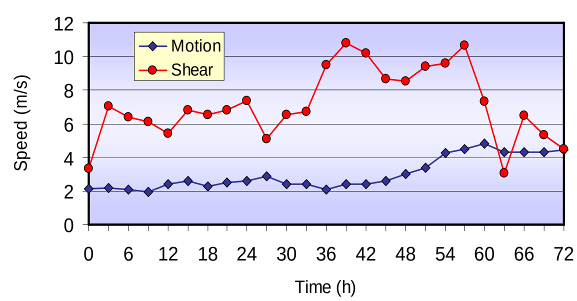

Figure 9: Time series of the magnitude of the tropical cyclone motion and environmental shear for the variable-*f* simulation.

The brief period of shear greater than 10 m s^{-1} is associated with a brief period of non-intensification of the tropical cyclone, which lags the shear onset by about 6 hours (Fig. 1). The direction of the shear is generally to the south-southeast or southeast, which is consistent with the downshear-left location of the rainfall asymmetry in Fig. 5d. Although the magnitude of the shear changes quite substantially between 24 and 72 hours of simulation, the strength of the 850 mb jet changes very little. As stated earlier, it is the upper-levels of the tropical cyclone that change significantly, changing the value of shear over the tropical cyclone.

3.4 Some implications of the variable-f vertical wind shear

Figure 10 shows the 48-h, 500-mb asymmetric component of the flow over a comparable "dry" variable-*f* simulation in which the cloud-resolving parameterization is turned off. The beta gyres tend to be masked in the moist simulations by asymmetries associated with the strong convective updrafts. It can be seen in Fig. 10a that the strongest part of the flow is right over the tropical cyclone center. Farther out from the center the asymmetric flow is still present, but is much weaker. Thus, the best estimate of the vertical wind shear associated with the beta gyres is that which includes the inner portion of the tropical cyclone. In this study, we used the inner 300 km because that was the area that also provided the best steering vector match to the actual simulated tropical cyclone motion. There are two issues when doing this calculation with standard large-scale analyses. Figure 10a shows the asymmetric component of the 500 mb wind

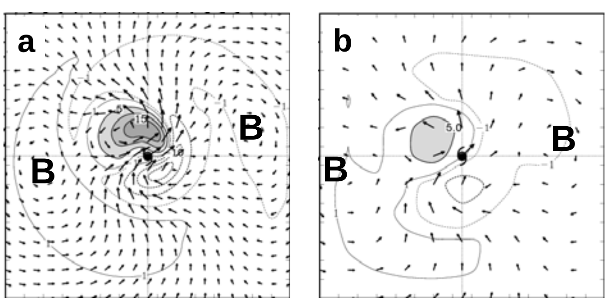

Figure 10: The 48-h, 500-mb asymmetric component of the wind field and relative vorticity for the dry variable-*f* simulation for: a) the original 15-km resolution domain; and b) degraded to 180-km resolution. The domains shown are 1200 x 1200 km, and the beta gyres are indicated with a "B".

field at 48 h and 15-km resolution, and Fig. 10b shows the same field degraded to 180-km resolution. From Figure 10b it can be seen that even if perfect grid point observations were available at this resolution, they would barely resolve the asymmetric flow over the TC center due to the beta gyres. A second issue is the practice of bogussing a vortex into the large-scale analyses based on an intensity estimate and radius of gale-force winds. Although some systems will include an asymmetric component of wind to match initial motion of the tropical cyclone, they may not include a vertical structure to the motion that will match the beta-gyre shear. Thus, large-scale analysis fields will most likely represent the basic flow patterns of the environment, but it is unlikely that they will adequately represent the "beta shear" discussed here.

The vertical wind shear calculated over the inner 300-km radius of the tropical cyclone becomes quite strong (> 8 m s^{-1}) for a portion of the simulation before relaxing back to about 5 m s^{-1} by 72 h of simulation. As discussed by Frank and Ritchie (2002), the direction of shear is consistently to the south-southeast or southeast indicating a small bias in zonal direction that may well help to explain why there might be an east-west directional bias for favorable tropical cyclone genesis/intensification conditions (e.g., Tuleya and Kurihara 1981). That is, a 10 m s^{-1} large-scale easterly shear vector will add to a northeast beta shear vector of 8 m s^{-1} for a resultant north-northeasterly shear vector over the TC of 7.1 m s^{-1}. In contrast, a 10 m s^{-1} westerly shear vector will add to a northeast beta shear vector of 8 m s^{-1} for a resultant west-northwesterly shear vector over the TC of 16.7 m s^{-1} as demonstrated in Fig. 11. Much smaller amounts of environmental shear also result in large differences in the effective vertical wind shear influencing the tropical cyclone depending on whether they are easterly or westerly. The implications of 1) the magnitude and direction of the beta shear; and 2) the likelihood that large-scale analyses do not adequately capture this effect, are that, all other effects aside, the effective shear over a tropical cyclone will be much smaller in easterly shear environments than westerly shear environments for the same measured magnitude of environmental shear. Thus, a preference for intensification under easterly shear than westerly shear of the same magnitude will be apparent.

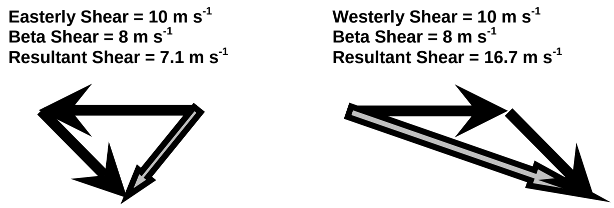

Figure 11: Schematic of the way the beta shear adds to an environmental vertical wind shear to produce a resultant shear over the tropical cyclone. According to this idea, a tropical cyclone embedded in easterly environmental vertical wind shear will always be favored to intensify over a TC embedded in the same magnitude of westerly vertical wind shear.

4. Summary and Discussion

Two simulations of a tropical cyclone are compared in order to understand the resulting differences in structure and intensity due to *in situ* shear that develops in a variable-*f* environment compared with a constant-*f* environment. Intensity is tracked through the minimum sea-level pressure rather than through the strongest surface winds. It is found that the tropical cyclone with variable *f* intensifies slightly more slowly than that with constant *f*, and reaches a final intensity that is about 5 mb weaker than the constant-*f* comparison. Both tropical cyclones reach an intensity that is within 20 mb of their predicted MPI based on the mean temperature sounding and SST.

There are some differences in the development of the wind fields between the two simulations. Whereas the constant-*f* TC maintains a relatively axisymmetric wind structure throughout the simulation, the variable-*f* TC develops a strong wind asymmetry in the northeast quadrant consistent with a movement toward the northwest. The main RMW contraction for the constant-*f* TC occurs between 54 and 60 hours of simulation and occurs through the 700 – 200 mb layer. Thus, the eyewall structure changes from a steep slope at 48 h to a much more upright eyewall by 72 h of simulation (Figs. 2b, 2c). In contrast, the main RMW contraction for the variable-*f* TC occurs between 24 and 48 hours of simulation at all levels. Subsequent to this, the RMW expands again as the TC structure becomes more asymmetric and moves to higher latitudes.

The spatial pattern of precipitation for the VFTC also exhibits a more asymmetric structure than the CFTC simulation with consistently higher rainfall in the eastern sector of the storm, as well as a rainband to the south. Both tropical cyclones produce about the same amount of total rainfall when averaged over a 300-km circle, but the CFTC has most of its rainfall concentrated within an intense eyewall. There are periods of stronger and weaker rainfall during the simulation period that correspond to fluctuations in both the minimum sea-level pressure, and environmental vertical wind shear over the TCs.

In spite of there being no forced environmental shear in either of the two simulations discussed here, vertical wind shear develops in both cases. The vertical wind shear that develops in the CFTC case is light and variable, and vertical profiles of the averaged wind indicate that the variability occurs in the upper-level outflow layer of the tropical cyclone. However, it is noted that when the vertical wind shear (measured as the difference between the average winds at 200 mb – 850 mb) is greater than 2.67 m s^{-1}, then associated eyewall rainfall asymmetries are observed in the hourly precipitation maps. Thus, rainfall asymmetries can develop under extremely light shear conditions and if persistent enough, may affect the rate at which the tropical cyclone intensifies.

The environmental vertical wind shear that develops in the variable-*f* simulation is quite substantial and ranges in value through the simulation from about 7 – 12 m s^{-1}. However, it is noted that the averaged winds below approximately 400 mb change little throughout the simulation. Thus, the majority of the changes in the calculated vertical wind shear is probably due to fluctuations in the more unstable outflow layer of the TC as proposed by Wong and Chan (2004). However, despite these fluctuations, the shear magnitude correlates fairly well with trends in the intensification of the TC with higher values of shear corresponding to less rapid intensification or even periods of no intensification (e.g., 39 – 48 h).

The direction of shear in the variable-*f* storm is consistently to the south-southeast or southeast indicating a small bias in zonal direction that may well help to explain why there is an east-west directional bias for favorable tropical cyclone genesis/intensification conditions. The beta shear will subtract from (add to) a basic easterly (westerly) shear to reduce (increase) the overall effective shear over the tropical cyclone. Because it is not clear whether the basic beta-gyre environment is adequately represented in observational analyses, this important effect may be missing from calculations of the environmental vertical wind shear in practice. An additional effect is that a weak southeasterly environmental shear could act to cancel the shear due to the beta gyres resulting in an effective zero-shear environment. Such an environment would be conducive to the development of very axisymmetric tropical cyclones similar to that in the constant-*f* simulation with almost no asymmetries in their rainfall patterns and the potential to intensify near their MPI. These may be the conditions under which annular hurricanes form (Knaff et al. 2003). Future work includes extending the analysis to include the effects of moderate to large vertical wind shear on tropical cyclone structure in variable *f*, and investigating the anomalous conditions under which annular hurricanes form.

Acknowledgments: The MM5 model was made available through the National Center for Atmospheric Research (NCAR). Part of this research was conducted while the second author was on sabbatical at the University of New Mexico. A manuscript based on these results has been submitted to *Monthly Weather Review* for consideration. All simulations and diagnostics were performed on the computers at the Center for High Performance Computing at the University of New Mexico. This research was sponsored by the National Science Foundation Physical and Dynamic Meteorology Program under Grant #ATM-0209416.

References:

Bender, M. A., 1997: The effect of relative flow on the asymmetric structure of the interior of hurricanes. *J. Atmos. Sci.,* **54,** 703-724.

Chan, J. C. L., and R. T. Williams, 1987: Analytical and Numerical Studies of the Beta-Effect in Tropical Cyclone Motion. Part I: Zero Mean Flow. *J. Atmos. Sci.,* **44,** 1257–1265.

Fiorino, M., and R. L. Elsberry, 1989: Some Aspects of Vortex Structure Related to Tropical Cyclone Motion. *J. Atmos. Sci.,* **46**, 975–990.

Frank, W. M., and E. A. Ritchie, 2001: Effects of Vertical Wind Shear on Hurricane Intensity and Structure. *Mon. Wea. Rev.,* **129**, 2249-2269.

Gray, W. M., 1975: Tropical cyclone genesis. *Dept. of Atmos. Sci. Paper No. 234, Colo. State Univ., Ft. Collins, CO,* 121 pp.

Halverson, J., G. M. Heymsfield, J. Simpson, H. Pierce, T. Hock, and E. A. Ritchie, 2006: Warm core structure of Hurricane Erin diagnosed from high altitude dropsondes during CAMEX-4. *J. Atmos. Sci.,* **63,** 309-324.

Jones, S. C., 1995: The evolution of vortices in vertical shear. Part I: Initially barotropic vortices. *Quart. J. Roy. Meteor. Soc.,* **121,** 821-851.

Knaff, J. A., J. P. Kossin, and M. DeMaria. 2003: Annular Hurricanes. *Weather and Forecasting*, **18**, 204–223.

McBride, J. L., and R. M. Zehr, 1981: Observational analysis of tropical cyclone formation. Part II: Comparison of non-developing vs. developing systems. *J. Atmos. Sci.,* **38,** 1132-1151.

Tuleya, R. E., and Y. Kurihara, 1981: A numerical study on the effects of environmental flow on tropical cyclone genesis. *Mon. Wea. Rev.,* **109,** 2487-2506.

Wong, M. L. M., and J. C. L. Chan, 2004: Tropical Cyclone Intensity in Vertical Wind Shear. *J. Atmos. Sci*., **61**, 1859–1876.